JCTC Journal of Chemical Theory and Computation

Article

pubs.acs.org/JCTC

Exploring the Dynamic Functional Landscape of Adenylate Kinase Modulated by Substrates

Yong Wang,[†] Linfeng Gan,[†] Erkang Wang,[†] and Jin Wang*[,†,‡,§]

[†]State Key Laboratory of Electroanalytical Chemistry, Changchun Institute of Applied Chemistry, Chinese Academy of Sciences, Changchun, Jilin, 130022, P.R. China

[‡]College of Physics, Jilin University, Changchun, Jilin, P.R. China

[§]Department of Chemistry and Physics, State University of New York at Stony Brook, Stony Brook, New York 11794-3400, United States

Supporting Information

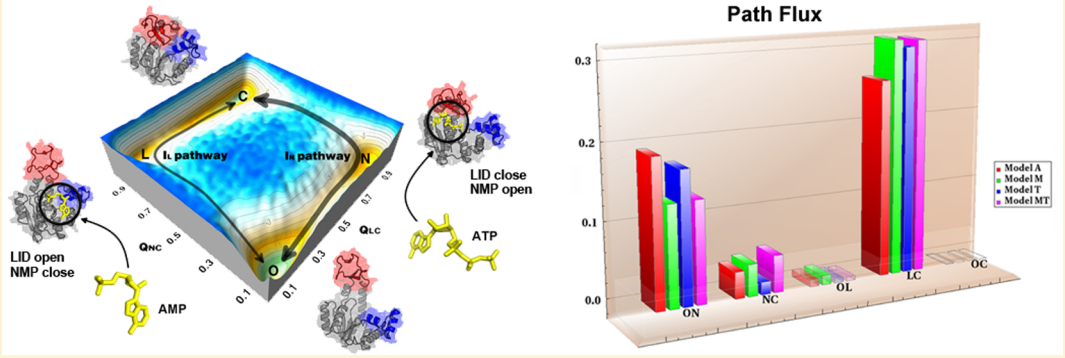

ABSTRACT: Adenylate kinase (ADK) has been explored widely, through both experimental and theoretical studies. However, still less is known about how the functional dynamics of ADK is modulated explicitly by its natural substrates. Here, we report a quantitative study of the dynamic energy landscape for ADK responding to the substrate binding by integrating both experimental investigations and theoretical modeling. We make theoretical predictions which are in remarkable agreement with the single molecule experiments on the substrate-bound complex. With our combined models of ADK in its apo form, in the presence of AMP or ATP, and in complex with both substrates, we specifically address the following key questions: (1) Are there intermediate state(s) during their catalytic cycle and if so how many? (2) How many pathways are there along the open-to-closed transitions and what are their corresponding weights? (3) How do substrates influence the pathway weights and the stability of the intermediates? (4) Which lid's motion is rate-limiting along the turnover cycle, the NMP or the LID domain? Our models predict two major parallel stepwise pathways and two on-pathway intermediates which are denoted as I_N (NMP domain open while LID domain closed) and I_L (LID domain open and NMP domain closed), respectively. Further investigation of temperature effects suggests that the I_N pathway is dominant at room temperature, but the I_L pathway is dominant at the optimal temperature. This leads us to propose that the I_L pathway is more dominant by entropy and I_N pathway by enthalpy. Remarkably, our results show that even with maximum concentrations of natural substrates, ADK still fluctuates between multiple functional states, reflecting an intrinsic capability of large-scale conformational fluctuations which may be essential to its biological function. The results based on the dual-ligands model provide the theoretical validation of random bisubstrate biproducts (Bi−Bi) mechanism for the enzymatic reaction of ADK. Additionally, the pathway flux analysis strongly suggests that the motion of the NMP domain is the rate-determining step for the conformational cycle (opening and closing).

INTRODUCTION

Biomolecules carrying out their functions are often accompanied by large-scale conformational changes.[1,2] These conformational changes can be induced by the binding of biomolecules, such as proteins, DNA, or ligands.[3] It is a subject of great interest to explore the relationship between conformational dynamics and biological functions,[4,5] particularly the interplay between functional dynamics and ligand binding.[6,7] In the study of enzyme dynamics−function relationships, adenylate kinase (ADK) has attracted much attention and is considered an excellent model system.

ADK catalyzes the reversible phosphoryl transfer reaction, $Mg^{2+}ATP + AMP \rightarrow Mg^{2+}ADP + ADP$. This is found to be ubiquitously present in many different organisms from all three kingdoms of life.[8] The enzyme is recognized to be essential for maintaining the energy balance by regulating the concentration

Received: August 15, 2012
Published: November 5, 2012

 © 2012 American Chemical Society

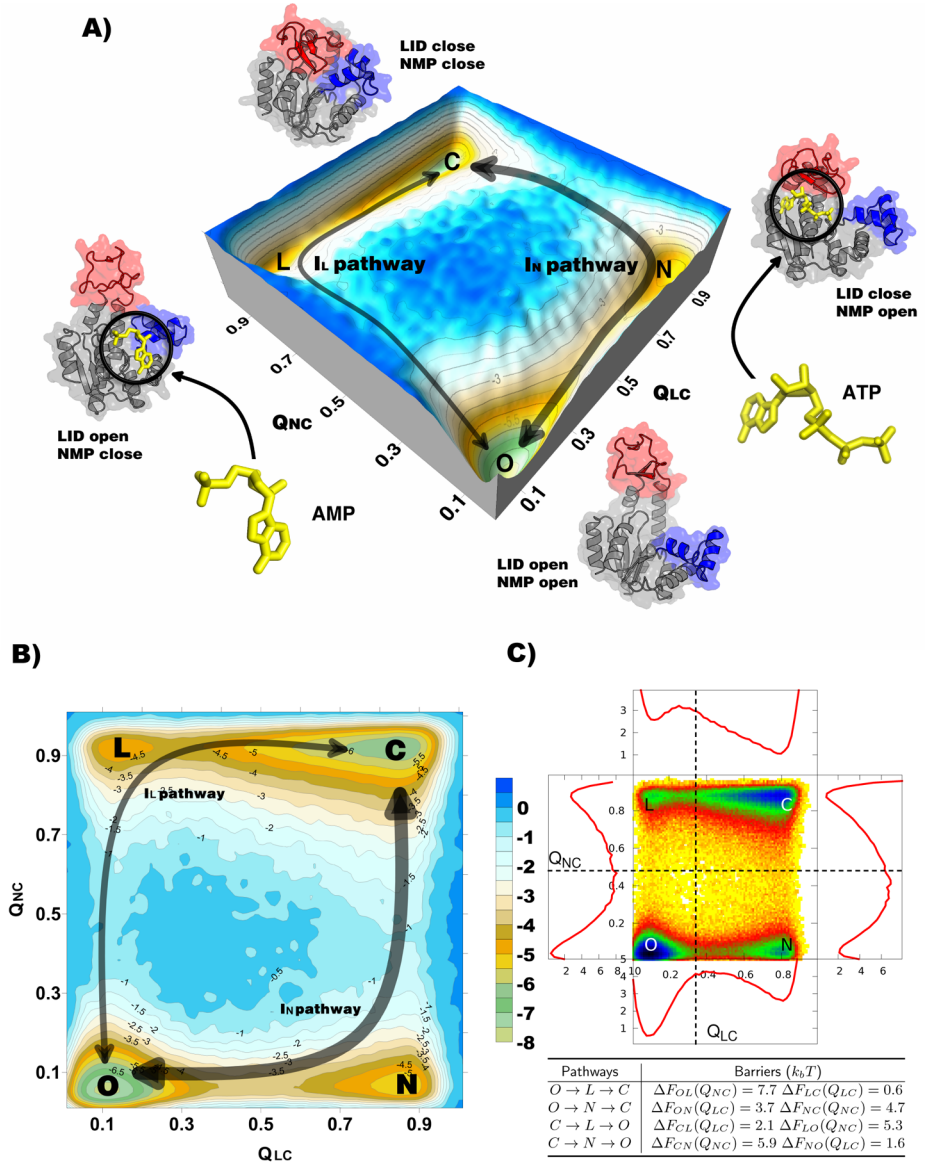

Figure 1. Free energy surface $F(Q_{LC},Q_{NC})$ indicates two intermediates and two parallel pathways (model A). Q_{LC} and Q_{NC} represent the fraction of specific native contacts between the LID domain and the CORE domain and between the NMP domain and CORE domain, respectively. There are four free energy basins. The O and C basins represent the full open state and the full closed state, respectively. One intermediate state in the N basin (denoted as I_N) represents the conformational ensemble where the LID domain is closed but the NMP domain is open. Another one in the L basin (denoted as I_L) represents the conformational ensemble where the LID domain is open but the NMP domain is closed. The two intermediates connecting the O and C basins yield two major parallel pathways. The corresponding paths passing I_N and I_L are denoted as the "I_N pathway" and the "I_L pathway", respectively. (C) The free energy barriers were measured by a strategy that splits the profiles. The barriers between the O basin and the N basin were calculated from the conformational region of $Q_{NC} < 0.5$. The region $Q_{NC} > 0.5$ is used to measure the barriers between the L basin and C basin. In addition, the barriers between the O basin and the L basin are measured according to the conformational region $Q_{LC} < 0.35$; the C−N barriers are according to $Q_{LC} > 0.35$. Note that free energy barriers are in unit of k_BT, where k_B is the Boltzmann constant.

of free adenylate nucleotides within the cell. Its misfunction may lead to human health issues such as hemolytic anemia and coronary artery disease.[9] Typically, ADK consists of three domains: a CORE domain, an ATP-binding (LID) domain, and an AMP-binding (NMP) domain. The LID and NMP domains are both highly dynamic on a wide range of time scales[10] and undergo significant conformational changes in response to substrate binding.[11,12] It is evident that the large-scale conformational changes can even occur in the absence of ligands.[13] This rearrangement of the two mobile domains is necessary for the accommodation of nucleotides in an optimal catalytic geometry.

More recently, there has been a variety of experiments and computer simulations carried out for ADK;[8,10,14−28] however, a complete understanding of the mechanism is still lacking. A number of fundamental questions remain generally unanswered: What is the order of LID and NMP domain opening/closure? Do intermediate state(s) exist during their catalytic cycle? If so, how many are there? How many pathways are there along the open/close transitions? Are these pathways different in the absence and the presence of ligands? Both structural and biophysical studies have suggested that large-amplitude interconversion between inactive (open) and active (closed) conformations is the rate limiting step for catalysis.[10,14]

dx.doi.org/10.1021/ct300720s | J. Chem. Theory Comput. 2013, 9, 84−95

It is directly determined by the large-scale fluctuations of the NMP domain (AMP binding lid) and the LID domain (ATP binding lid), whereas the CORE domain is remarkably stable during the allosteric transitions.[29−31] However, it is still a topic of debate which lid's motion is the rate-limiting step.[13,16,17,27]

Capturing the dynamics between various functional states is essential to understanding how such biological systems work. So far, it is still a challenge for experimentalists to directly obtain global time-dependent functional dynamics at high resolution. This prompted a number of theoretical efforts, especially for ADK, focusing on accelerating the dynamics and sampling of rare events. These approaches include elastic networks,[32] dynamic importance sampling,[8] minimalist plastic networks,[2,33] standard MD,[10,13,34] the TEE-REX algorithm,[35] distance replica exchange,[15] essential dynamics sampling,[36] targeted Monte Carlo,[37] normal-mode analysis with simplified elastic networks,[17,20] and minimum free energy path.[28] In particular, it has become increasingly apparent in recent years that theorists investigated the functional dynamics at the bottom of the funneled landscape using coarse-grained structure-based models, including the macroscopic[21,38,39] and microscopic multibasin models,[19,40,41] and also the microscopic mixing contact map.[16,42,43] These models have provided extraordinary insights into the kinetic and energetic details of these allosteric transition processes, as well as a validation of energy landscape theory.[5] These coarse-grained models approximate the effects of ligand binding implicitly by an effective two-body residue−residue contact interactions in a protein mediated by ligand(s).

In the present work, we developed a new structure-based functional model by introducing explicit ligands which typically were ignored or implicitly considered in previous coarse grained models. Explicit modeling of ligands can naturally take into account of the interactions between the protein and ligands. It is not only important to monitor more realistically and accurately the detailed process of functional motion and transition but also critical for the investigations of the functional landscape responding to ligand binding. Moreover, our model also represents an exciting opportunity to check and validate the random Bi−Bi mechanism for the enzymatic reaction of ADK, which is a long-standing question in the community. To specifically address these aforementioned questions for ADK, we employed a combination of four models: (1) model A which represents ADK in its apo (ligand-free) form, (2) model M in the presence of AMP, (3) model T in the presence of ATP, and (4) model MT in complex with both ligands. Our results based on these models lead to the next level understanding of the functional dynamics of ADK modulated by its natural substrates. In particular, the combination of these models is able to predict the dynamic functional landscape in response to ligand binding and temperature change consistent with single molecule experiments.

RESULTS AND DISCUSSION

To reach the efficient catalytic efficiency, ADK is required to maintain fast fluctuations between different unique conformational substates. For example, it requires open conformations for capturing the reactants (AMP and ATP) and releasing the products (two ADPs) and closed conformations for the formation of the precise catalytic geometry. Recent studies have been accumulating evidence that ADK is capable of executing large-scale conformational fluctuations even without a ligand.[13] In other words, both LID and NMP domains can close the active site in the apoenzyme (Figure 1A). More surprisingly, the single-molecule experiment reveals that the equilibrium of the LID domain favors the closed conformation in the absence of substrates.[13] On the basis of these experimental measurements, we first explore the fundamental mechanism of the intrinsic conformational fluctuations by using the apo-ADK model (model A). As detailed in the section Methods and Models in the Supporting Information (SI), we used coarse-grained C_A-C_B/C_P chains to model ADK and ligands. Different from previous models,[16,19,21,38,39] the ligands (including AMP and ATP) are explicitly considered in the present work.

The apo-ADK Model. After determining the robustness of our model by a series of parameter tests (see Tests of Parameters in the SI), we calibrated the ε_1 and ε_2 (ε_1 is the strength of the share contacts and ε_2 is the strength of the state-specific contacts) so that the relative population of open (O) and closed (C) states in substrate-free simulation is comparable to experimental measurements of the single-molecule FRET carried out by Hanson et al.[13] From the single-molecule observation, it clearly demonstrates that ADK is capable of stochastically sampling a wide range of conformations on the millisecond time scale, even without its substrates.[13] By analyzing the results (Figure 2C in ref 13) of the conformational distribution of substrate-free ADK, the study reveals that the closed population (in fact, the LID-closed) from the experimental measurement is in the range of 40%−90%. Note that the error is mainly due to uncertainties from the open−closed rate measurements. To draw comparisons from the FRET experiment, we employed the distance between A127 in LID and A194 in CORE ($R_{L_{127}C_{194}}$) as a reaction coordinate (RC) to monitor the motion of the LID domain relative to the CORE domain. It is worthwhile pointing out that this RC remains a minor difference between the simulation and the experiment, because the latter employed the distances between the transition dipole of the two dyes. Parameter set $\varepsilon_1 = 2.0$ and $\varepsilon_2 = 1.2$ results in a LID-closed conformation with a population

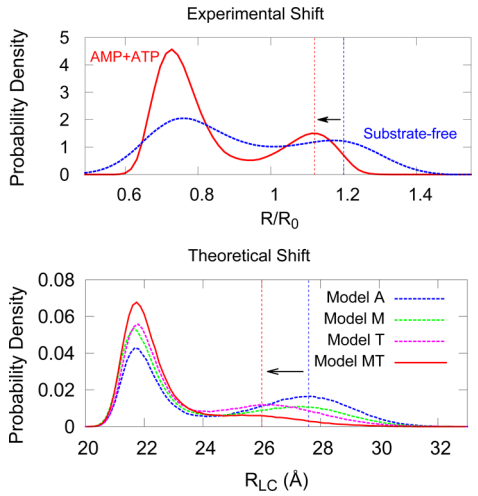

Figure 2. Shift of conformational distributions. The shift of conformational distributions is measured by the distance between center of mass of LID and CORE (R_{LC}). It shows the experimental measurement of probability distributions for substrate-free ADK and ligand-bound enzymes with AMP and AMP−PNP, and simulated measurement of probability distributions for model A, model M, model T, and model MT.

dx.doi.org/10.1021/ct300720s | J. Chem. Theory Comput. 2013, 9, 84−95

of about 50%, which is in the region of experimental measurement. The conformational probability distribution is plotted as a function of $R_{L_{127}C_{194}}$ and fit with experimental distribution (Figure S5A in the SI).

These parameters yield a ratio of strength for state-specific contacts to strength for core contacts of 0.6. We found that the model works well, as the ratio was between 0.5 and 0.65. It suggests that the state-specific contacts are significantly weaker than the shared contacts, which is also found in other allosteric systems.[38,43] This allosteric feature is likely incorporated to facilitate large-scale conformational changes by switching only partial key contacts.

On the basis of the calibration, we first investigated the free energy surface as a function of $RMSD_O$ (RMSD to open crystal structure) shown in Figure S5B in the SI. It clearly indicates that there is at least an intermediate state that exists between the native open and closed states. By monitoring the compactness (quantified by radius of gyration) of all three domains in the molecular dynamics simulation, it was found that the conformational fluctuation in ADK is mainly due to the interdomain displacement and not from the intradomain conformational change.[24,31] Because the RMSD is only a global RC which may miss the fluctuations of individual domains, we introduce other RCs to measure the motion of the LID and NMP domains. Next, we explore the intermediate state by performing the analysis of multidimensional free energy profiles (Figure S6 in the SI).

The free energy surface as a function of Q_{LC} (the fraction of native interfacial contacts between LID and CORE domain) and Q_{NC} (the fraction of native interfacial contacts between NMP and CORE domain) is shown in Figure 1B. Note that we chose these RCs because they have been successfully used in many folding and allosteric simulations.[8,31,44,45] It clearly shows that there are two intermediates in the free energy surfaces in addition to one fully open state and one fully closed state which are explicitly integrated into the structure-based model. One intermediate state (denoted as I_N in the N basin) represents the conformation ensemble where the LID domain is closed but the NMP domain is open. Another one (denoted as I_L in L basin) represents the conformation ensemble where the LID domain is open but the NMP domain is closed. In fact, more specifically, the LID domain in intermediate L is partially closed (Figure S6). The two intermediates connecting the O and C basins yield two major parallel pathways. The corresponding paths passing I_N and I_L are denoted as the "I_N pathway" and the "I_L pathway", respectively.

From Figure 1, we can see that I_N locates at a deeper free energy basin than I_L does, and both intermediates have shallower basins than those of the O and C states. At the current simulated temperature, their conformational weights are both less than 11%. The low conformational weight may be the reason that the two intermediates were hard to detect in previous experiments.

The two intermediates connecting the open and closed basins yield two major pathways. Due to the complexity of the functional landscape for ADK, the one-dimensional free energy profile has a hard time characterizing the conformational transitions between the four energy basins and is unable to measure the free energy barriers between them. We employed a strategy that splits the two-dimensional free energy surface. In this way, we can measure the free energy barriers between the O basin and N basin from the free energy profile as a function of Q_{LC} in the conformational region of $Q_{NC} < 0.5$. Similarly, the O−L barriers are measured from the free energy profile as a function of Q_{NC} in the region of $Q_{LC} < 0.35$. The results are summarized in Figure 1C. The free energy barrier from the A basin to the B basin is denoted as $\Delta F_{AB}(X)$ which is measured from the profile as a function of X. For example, $\Delta F_{OL}(Q_{NC})$ is the O→L barrier from the free energy profile as a function of Q_{NC}. By comparison of $\Delta F_{ON}(Q_{LC})$ and $\Delta F_{LC}(Q_{LC})$, it shows that the barrier height for the LID closing is $3.7k_BT$ as the NMP is opening; however, it decreases to $0.7k_BT$ upon NMP closing. In addition, $\Delta F_{OL}(Q_{NC})$ and $\Delta F_{NC}(Q_{NC})$ indicate that the barrier heights for NMP closing are $7.7k_BT$ upon LID opening and $4.7k_BT$ upon LID closing, respectively. Significantly, the barrier of closing one domain decreases dramatically (up to $3k_BT$) as another domain closes. The further analysis for the open direction also supports that the preceding opening of NMP lowers the barrier of LID opening with $0.5k_BT$ ($\Delta F_{CL}(Q_{LC}) = 2.1k_BT$ and $\Delta F_{NO}(Q_{LC}) = 1.6k_BT$), and opening of LID lowers the barrier of NMP opening with $0.6k_BT$ ($\Delta F_{CN}(Q_{NC}) = 5.9k_BT$ and $\Delta F_{LO}(Q_{NC}) = 5.3k_BT$). Taken together, it leads to the conclusion that the preceding movement of one domain facilitates the fluctuation of another domain, especially for the closing direction. In other words, ADK applies a stepwise mechanism with two on-pathway intermediates to the open or closed conformation. In contrast, the simultaneous opening/closing mechanism is highly unfavored, which is evident from the kinetic analysis and the following flux analysis.

In Figure 1C, we also noticed that the barriers for O ↔ L and N ↔ C transitions were higher than that for O ↔ N and L ↔ C transitions. This indicates that the motion of the LID domain has a relatively lower barrier to that of NMP. This also implies that the rate-limiting step for the conformational change cycle may be related to the motion of the NMP domain rather than the LID domain. We will give a detailed analysis of the rate-limiting step in the following section (Rate Description and Flux Description of Pathways).

The finding that there are lower barriers associated with LID motion than with NMP motion for both opening and closing directions is also supported by previous works;[16,19,42] however, it does not necessarily lead to the conclusion that the I_L pathway is dominant for both directions. The most rigorous and accurate way is to quantify the weight of multiple possible pathways, such as using flux description analysis. It is important to emphasize that some possible kinetic pathways may be hidden in free energy profiles which have been identified in previous studies of ours,[43] although the free energy profiles can provide useful thermodynamic information.

The Ligand-Binding Models. There is mounting evidence that these conformational fluctuations must be influenced in the presence of the ligands. However, experimentally it is still difficult to address the detailed effect of ligands in conformational fluctuations at a microscopic level.[13] In this work, we carried out the molecular dynamics simulations through a combination of three explicit-ligand models consisting of two ligand-binding models (models M and T) and their combination model MT (see Table S1 in the SI) to investigate the effects of different ligands interacting with ADK. We calibrate the parameters of the strength of ligand binding (ε_{AMP}, ε_{ATP}) so that the disassociation equilibrium constants are comparable to the experimental data.[9,13,18,46] With $\varepsilon_{AMP} = 1.1$ and $\varepsilon_{ATP} = 1.5$, the disassociation constants of AMP and ATP are $K_D^{AMP} = 195.3\mu M$ and $K_D^{ATP} = 31.0\ \mu M$.

dx.doi.org/10.1021/ct300720s | J. Chem. Theory Comput. 2013, 9, 84−95

The probability distributions of the LID-CORE distance (R_{LC}) with and without ligands summarized from the FRET experiment and our simulation are shown in Figure 2. By comparing them with experimental measurements in conformational redistribution, it is shown that the theoretical results fit well with experimental findings, including not only the increase of the closed peak but also the shift of the open peak in the presence of ligands. It can further confirm that the shift of the open peak is from ADK's interaction with ligands, which is consistent with previous experiments.[47,48]

The explicit consideration of ligands provides us an exciting opportunity to characterize explicitly the conformational change mechanism of ADK responding to ligand binding. There are, at present, two distinct mechanisms that have been suggested to describe the conformation transitions in biomolecular recognition. The first is called induced fit.[49,50] The second proposed mechanism is called conformational selection or population shift.[5] Under the framework of energy landscape theory, the boundary between the two mechanisms is not necessarily so distinctly clear. Even the induced fit can be considered a limiting case of conformational selection (the interaction partner selectively binds to the pre-existing inactive conformation).[49,51] Our models support the view that the closed state is already sampled in the substrate-free enzyme; the binding of the substrates does not induce the formation of a new conformational state but instead shifts the population of pre-existing states.[49,50] However, we have to emphasize that it does not necessarily mean a population shift scheme for the conformational change of ADK. In order to clearly describe the mechanism of conformational change for ADK, the conventional definitions are used here. "Induced fit" means that ligand binding drives a ligand-free (usually open) enzyme toward the activated conformation (usually closed). "Population shift" means that the unbound protein takes on multiple functional states (including the activated state). Subsequently, ligands selectively bind to the pre-existing activated conformation. Using these definitions, the induced fit and conformational selection paradigms represent the two extremes of the possible mechanisms.

In particular, our double-ligand model MT allows us to validate the bisubstrate biproducts (Bi−Bi) reaction mechanism. It will be discussed in greater detail in the Discussion section.

Effects of Ligand Binding. First, we investigate the effect of ligand-binding strength on the population distribution of ADK by a variety of ε_{AMP} and ε_{ATP} from 0.0 to 2.0. The results are summarized in Figure S7 in the SI. It indicates that the population of the closed state increases dramatically as the strength of the AMP or ATP binding increases, while the population of the open state decreases in unison. The relationship between ligand-binding strengths and pathway weights indicates that the weight of the I_N pathway decreases with the increase of ε_{AMP} in model M. It is even more obvious for the I_L pathway that its weight decreases as the ε_{ATP} in model T increases. It is also expected that with high ligand-binding strength (ε_{AMP} or ε_{ATP} larger than 2.0), ADK will be almost fully locked in the closed state. This implies that the strength of the ligand-binding interaction, or in the other words the affinity between ligand and its target enzyme, plays an important role of closing the enzyme and also the conformational redistribution. NMR and X-ray experiments have suggested that ADK is fully closed in the presence of the tight-binding inhibitor AP5A.[14,47]

We next considered the response of conformational distribution and pathway weight to the variation of ligand concentrations (Figure 3). The further dependence on models

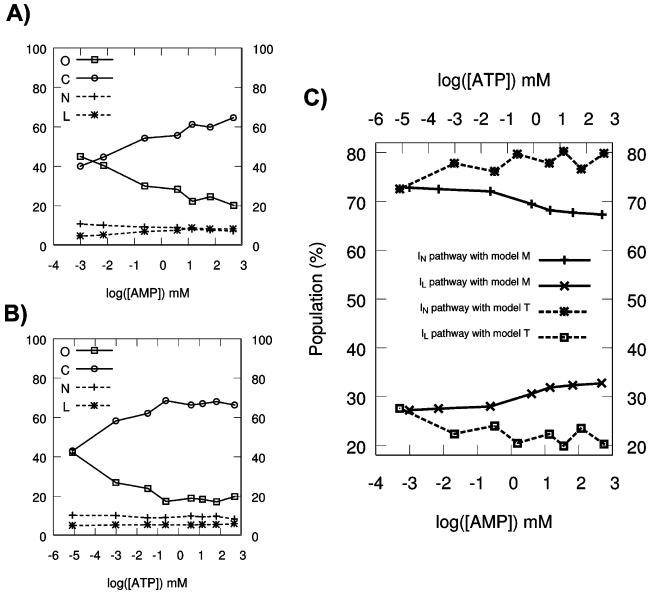

Figure 3. Relationships between ligand concentration and populations of states and pathways. We first calibrated the binding affinities of AMP and ATP under the condition of [AMP] = 0.5 mM and [ATP] = 0.5 mM by setting R_{AMP} and R_{ATP} to be 9.4 nm in the wall potential (see definition in the SI). R_{AMP} and R_{ATP} determine the volume of the reaction container for AMP and ATP in simulation. Then, the concentrations of ligands are modulated by changing R_{AMP} and R_{ATP} between 40.0 and 3.0 nm, corresponding to concentrations between 0.006 mM and 14.7 mM. (A) Populations of states as a function of AMP concentration with model M. (B) Populations of states as a function of ATP concentration with model T. (C) Comparison of pathway weights for models M and T.

is shown in Figure 4. It is clearly shown that the population of the closed state increases from 40% to 64%, and the population of the open state decreases to 20% as the concentrations of AMP and ATP increase. Additionally, it indicates that the increase of the closed population slows down with high ligand concentrations. In model MT, the limiting population of the C state is 75% (Figure 4A). In contrast, the closed population can reach up to more than 90% by increasing the ligand-binding strength (Figure S7 in SI). In other words, ADK is still capable of fluctuating between open and closed conformations in the presence of its natural substrates, even with the highest concentrations. Whereas the enzyme will be fully locked in the closed state if the ligand-binding interactions are strong enough. The dependence of pathway weights on ligand concentration is shown in Figure 3C. It indicates that increasing the concentration of AMP will decrease the weight of LID closing pathways, and an increase in the ATP concentration will increase the LID closing pathways. The pathway redistribution can be understood in terms of AMP and ATP's interactions with their respective lids; that is, AMP binding stabilizes the closed conformation of AMP lid (NMP), and ATP binding favors ATP lid (LID) closing. We have to mention the limitation of our model in which the non-native interactions between the AMP and LID domains are not considered, although there are experimental reports of LID closing in response to AMP binding.[18,52]

dx.doi.org/10.1021/ct300720s | J. Chem. Theory Comput. 2013, 9, 84−95

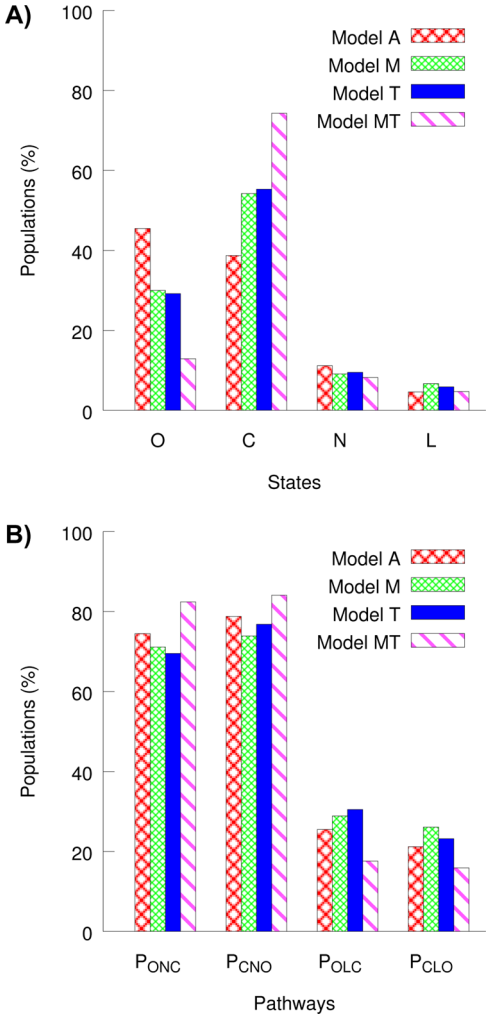

Figure 4. The dependence of basin stability and pathway weight on ligand-binding with different models. The ligands play an important role in modulating the population of basins (A); however they do not dramatically change the pathway weights (B) at the present temperature.

From the dependence of pathway weight on ligand affinity and ligand concentration, we may conclude that the ligands play an important role in modulating the energy landscape (the population of basins); however, they do not dramatically change the mechanism of conformational change (pathway weights) at the present temperature.

Rate Description and Flux Description of Pathways. Thermodynamic analysis reveals that the open and closed states of ADK on the free energy surface are linked by two intermediate states, and the interconversion proceeds along multiple pathways. This begs the following question: Which step is rate-limiting for the cycle of conformational change? To answer this question, we first calculate the rate constants to investigate the basin kinetics of the system by applying a method analogous to the one described in ref 53 that explored the folding free energy landscape of the Trp-cage miniprotein. We construct a reduced kinetic scheme by considering the transitions just between the native basins and intermediate states. The transition rate constants are estimated as the ratio of transition numbers to the total residence time in the starting basin. Then, we calculate the relative weight of a given path by computing the reactive flux through that route as suggested by Hammes et al.[54]

On the basis of the thermodynamic and kinetic simulation results, we constructed a four-state kinetic transition model, which was summarized in Figure 5A. Open and closed states are represented by labels O and C. The two intermediates I_N and I_L are labeled as N and L. The arrows point in the direction of the flux, and the transitions between two adjacent states are represented above or under the arrow. For example, transition from O to N is denoted as ON. NO means the reverse transition of ON from N to O. In principle, ADK opening and closure can go through three different pathways including the I_N pathways, I_L pathways, and direct pathways (along the diagonal line in Figure 5A). However our simulation reveals that the fluxes of direct transition pathways are negligible. Thus, the OC or CO routes are not considered in the kinetic analysis except where specified. For simplification, the four-state model does not distinguish the ligand-bound and ligand-free state.

Furthermore, the simulated rates are compared with the experimental rates measured by single-molecule FRET.[13] Considering that the experimental rates were actually measured according to the opening and closing of LID, we calculated the opening rate by $k_{open}^{simu} = k_{NO} + k_{CL}$ and the closing rate by $k_{close}^{simu} = k_{NO} + k_{CL}$. In Figure 5C and D, we can see that the rescaled simulation rates are in good agreement with experimental measured rates within errors, indicating that the effect of substrates on the transition rates is well reproduced in the simulation based on our explicit-ligand multibasin models. It also shows that k_{OL}, k_{LC}, k_{ON}, and k_{NC} from the open to closed direction increase from model A to model MT, indicating the lid closing rates increase upon binding with AMP or ATP. This is also consistent with the single molecule experimental observations,[13] suggesting the faster lid-closing rate upon binding of substrates. It also suggests that the opening rates are less influenced by the interactions with ligands.

Because there are three parallel pathways from C basin to O basin, the open rate can be calculated by

$$k_{open} = k_{CNO} + k_{CLO} + k_{CO}\ (\text{parallel}) \tag{1}$$

$$\approx k_{CNO} + k_{CLO}\ (k_{CO} \approx 0) \tag{2}$$

$$\approx \frac{1}{\frac{1}{k_{CN}} + \frac{1}{k_{NO}}} + \frac{1}{\frac{1}{k_{CL}} + \frac{1}{k_{LO}}}\ (\text{serial}) \tag{3}$$

$$\approx k_{CN} + \frac{1}{\frac{1}{k_{CL}} + \frac{1}{k_{LO}}}\ (k_{NO} \gg k_{CN}) \tag{4}$$

$$\approx k_{CN} + k_{LO}\ (k_{CL} \gg k_{LO}) \tag{5}$$

where k_{CNO} is the transition rate along the I_N pathway, and k_{CLO} is the transition rate along the I_L pathway. Because the direct transitions between O and C are rare, the term k_{CO} can be neglected. We then have eq 2 from eq 1. For a serial pathway, for example C → N → O, the transition rate constant is calculated by $k_{CNO} = 1/[(1/k_{CN}) + (1/k_{NO})]$. Then, we get eq 4 by considering $k_{NO} \gg k_{CN}$ (Figure 5B and D). It indicates that transition from C to N is the rate-limiting step for I_N opening pathway. Additionally, $k_{CL} \gg k_{LO}$ indicates that transition from from L to O is the rate-limiting step for the I_L opening pathway. On the basis of this, eq 4 can be further simplified as eq 5. The two terms in eq 5 added together give a

dx.doi.org/10.1021/ct300720s | J. Chem. Theory Comput. 2013, 9, 84−95

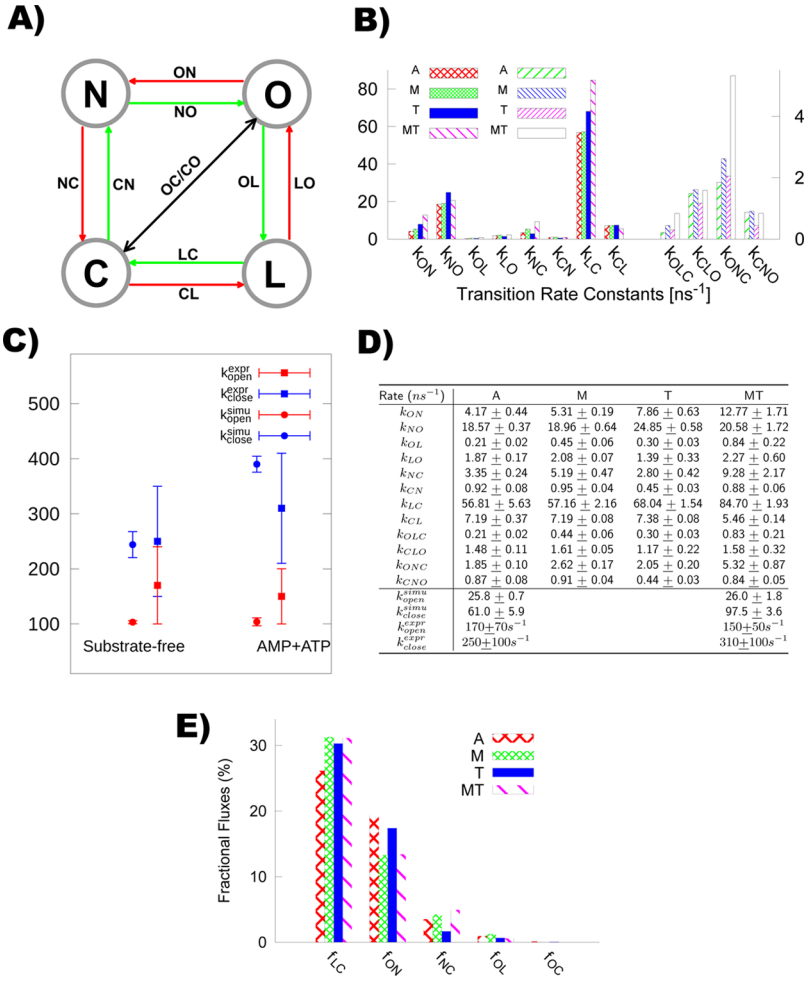

Rate (ns^{-1})	A	M	T	MT
k_{ON}	4.17 ± 0.44	5.31 ± 0.19	7.86 ± 0.63	12.77 ± 1.71
k_{NO}	18.57 ± 0.37	18.96 ± 0.64	24.85 ± 0.58	20.58 ± 1.72
k_{OL}	0.21 ± 0.02	0.45 ± 0.06	0.30 ± 0.03	0.84 ± 0.22
k_{LO}	1.87 ± 0.17	2.08 ± 0.07	1.39 ± 0.33	2.27 ± 0.60
k_{NC}	3.35 ± 0.24	5.19 ± 0.47	2.80 ± 0.42	9.28 ± 2.17
k_{CN}	0.92 ± 0.08	0.95 ± 0.04	0.45 ± 0.03	0.88 ± 0.06
k_{LC}	56.81 ± 5.63	57.16 ± 2.16	68.04 ± 1.54	84.70 ± 1.93
k_{CL}	7.19 ± 0.37	7.19 ± 0.08	7.38 ± 0.08	5.46 ± 0.14
k_{OLC}	0.21 ± 0.02	0.44 ± 0.06	0.30 ± 0.03	0.83 ± 0.21
k_{CLO}	1.48 ± 0.11	1.61 ± 0.05	1.17 ± 0.22	1.58 ± 0.32
k_{ONC}	1.85 ± 0.10	2.62 ± 0.17	2.05 ± 0.20	5.32 ± 0.87
k_{CNO}	0.87 ± 0.08	0.91 ± 0.04	0.44 ± 0.03	0.84 ± 0.05
k_{open}^{simu}	25.8 ± 0.7			26.0 ± 1.8
k_{close}^{simu}	61.0 ± 5.9			97.5 ± 3.6
k_{open}^{expr}	170±70s^{-1}			150±50s^{-1}
k_{close}^{expr}	250±100s^{-1}			310±100s^{-1}

Figure 5. Rate description and flux description of pathways. (A) Schematic diagram of the four-state conformational transition model. Open and closed states are represented by labels O and C. The two intermediates I_N and I_L are labeled as N and L. The arrows point in the direction of the flux. The transitions between two adjacent states is represented above or under the arrow. Green arrows represent the clockwise flux, and red arrows represent the counter-clockwise flux. The direct transition between paths between O and C are represented by a black double-head arrow. (B) Transition rate constants (in unit of ns^{-1}) with different ligand-bound models. (C) Simulated rates fit to experimental rates (in unit of s^{-1}). The rescaled simulated rates fit well with experimental data in the absence and presence of natural ligands. (D) Summary of the transition rate constants in the table. (E) The pathway fluxes in different models. Note that the clockwise fluxes (O → L → C → N → O) are almost equal to the counter-clockwise fluxes. On the basis of the flux symmetry, we only show the flux from A to B (denoted as f_{AB}) for clarity.

clear view that NMP opening is the rate-limiting step for both opening pathways.

Similarly, the closing rate of ADK is given by

$$k_{close} = k_{ONC} + k_{OLC} + k_{OC} \approx k_{ONC} \quad (6)$$

From Figure 5D, we can also find that the ratio of k_{OLC} to k_{ONC} is about 0.11. This directly leads to eq 6 being simplified into k_{ONC} (by ignoring k_{OLC}). Because k_{ON} is comparable to k_{NC}, both the rate of LID closing and the rate of NMP closing along the I_N pathway have a great impact on the total rate of ADK closing. In other words, the rate-limiting analysis gives the result that the two lids both play important roles in the conformational dynamics of ADK.

Next, we will investigate the conformational dynamics using flux description. Instead of absolute flux, we calculate the fractional flux, which is equal to the ratio of flux from A to B to the total flux of all possible paths. For example, the fractional flux from O to N is given by $f_{ON} = N_{ON}/(\sum N_{AB})$ (see details in SI). Note that N_{AB} is the transition number from A to B. A and B can be any pair of adjacent basins in Figure 5A. It is worth noting that for all transitions between adjacent basins, the transition number of the forward direction (A → B) approximates with that of the reverse direction (B → A), resulting in equality between the clockwise fluxes (O → L → C → N → O) and counter-clockwise fluxes. In other words, the reverse fluxes are exactly equal to the forward fluxes. The precise symmetry of the forward and reverse pathway implies sufficient sampling and equilibrium of the system. Then, we only show the forward flux for clarity. The fractional fluxes are summarized in Figure 5E. It shows that the direct flux between the O and C basins (f_{OC}) is very low (upper limit 0.1%), indicating that the simultaneous opening/closing of two lids is almost impossible for ADK. For instance, for a sequential pathway A → B → C, the total flux is calculated by $1/[(1/f_{AB}) + (1/f_{BC})]$,[54] so as to be determined by the lowest flux, that is, $f_{ABC} \approx \min(f_{AB}, f_{BC})$ as f_{AB} and f_{BC} are not comparable with each other. So, we have that $f_{ONC} \approx f_{NC}$ and $f_{OLC} \approx f_{OL}$. Also, $f_{CNO} \approx f_{CN}$ and $f_{CLO} \approx f_{CL}$, if we consider the symmetry of fluxes.[55] This supports the NMP opening being the flux-limiting step for both the I_N opening pathway and the I_L opening pathway, and NMP closing is the flux-limiting step for both the I_N closing pathway and the I_L closing pathway. In other words,

dx.doi.org/10.1021/ct300720s | J. Chem. Theory Comput. 2013, 9, 84−95

regardless of the opening or closing of ADK, the motion of the AMP lid is the flux-limiting step. It is the true rate-limiting step.

By comparison with the results of rate description and flux description, it seems that they are consistent with each other with respect to the limiting step for ADK opening; however, rate description fails to determine the limiting step for ADK closing. On the basis of this, we suggest using the flux description instead of traditional rate description to analyze the conformational change cycle, although the latter method can also provide useful information.

In addition, from our simulations, we suggest that there are no significant fluxes between the ligand bound and unbound states in the closed form. This finding may rule out the population shift mechanism and suggest an induced-fit type mechanism.

Temperature Effects. It is well established that the power of enzyme catalysis is sensitive to external conditions, such as pH, salts, substrate concentration, and also temperature. Specifically, we investigate the effects of temperature on the conformational change of ADK in this work.

Catalytic activity of ADK (from *mesophile Escherichia coli*) has been measured as a function of the temperature.[14] It was reported that ADK reached its maximal activity slightly below the denaturation temperature of 45 °C. The experimental kinetic data were measured at room temperature. At this temperature, ADK is about 7-fold less active than its maximal activity.[14] The melting temperature for mesoADK is 54 °C, corresponding to the simulated folding temperature T_f = 66 measured from the heat capacity curve (Figure S8 in the SI), which shows one major peak which is consistent with the result in a recent work.[56] Interesting, in another work of ours about the folding of a Y-family DNA polymerase, we also found that there is only one major peak in the heat capacity curve, although the associated four-domain protein has a complex, multistate folding landscape.[57]

In comparison with experimental results, we used the smallest values of k_{open} and k_{close} to approximate the catalytic rate constant k_{cat}.[19] From Figure S9 in the SI, it seems that the maximal activity temperature in the simulation is located at about T = 60 in which the transition rates reach maximum values. Beyond this temperature, the catalytic efficiency will decrease because of partially or totally melting of the enzyme. For determination of the simulated temperature comparable with the experimental condition, we compared the turnover number or k_{cat} under different temperatures and found that the activity of ADK at T = 35 is about 7-fold less than that at T = 60. It indicates that the simulated temperature T = 35 reasonably matches the experimental conditions. In addition, the free energy barriers between four states are highly dependent on temperature (Figure S10 in SI).

Furthermore, we investigate the effects of temperature on the conformational distribution and also the pathway weights. The results are summarized in Figure 6. It is clearly shown that increasing the temperature will increase the population of the open state and decrease that of the closed state. In addition, the populations of two intermediates also increase. From Figure 6B, we found a rather surprising result that the mechanism of conformational change was reversed as the temperature near the maximal activity temperature of enzyme. Considering that increases in temperature result in a reduction of free energy barrier in the entropy term ($-T\Delta S$), we propose that the I_L pathway is more entropically driven and the I_N pathway is more enthalpically driven. At lower temperatures, the free energy barrier is dominated by the enthalpy term. At high temperatures (relatively, must be lower than melting temperature), the free energy barrier becomes dominated by entropy.

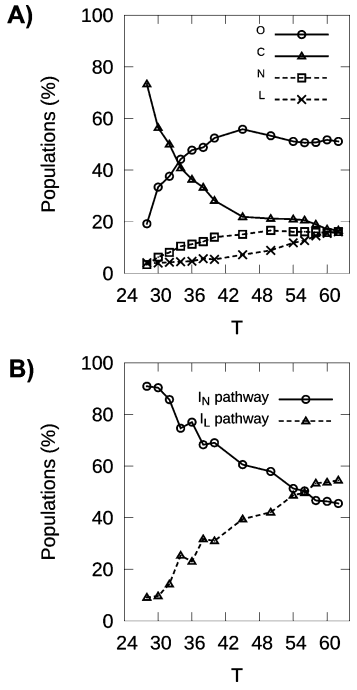

Figure 6. Temperature dependence of populations of states and pathways. (A) Increasing the temperature results in an increase of the population of the open state and a decrease in the population of the closed state. In addition, the populations of the two intermediates also increase. (B) The mechanism of conformational change is reversed as the temperature nears the maximal activity temperature of the enzyme, where the I_L pathway becomes slightly dominant.

Now, a question arises: will the rate-limiting step change at the maximal efficiency temperature? We re-examine it using the same method of the aforementioned flux description, as shown in Figure S11 in the SI. These results also support the conclusion that the motion of the AMP lid is still the flux-limiting step, which is consistent with simulations at lower temperatures.

DISCUSSION

Prediction of Intermediates. Previous simulations based on macroscopic potential of the whole system[2,21,39,41,58] were not capable of capturing the possible intermediate states except for predetermined states. Our model provides the capability of predicting the transition mechanism and intermediate states from a priori knowledge of structural information. The results also reflect that our model introduces the roughness of the underlying conformational energy landscape which is lacking in the macroscopic double-well potential models.[19,21] The landscape roughness is from the competition of attractive interactions from the structural topology of open and closed states.[19]

A search of available structures of ADK and its homologues from a variety of organisms resolved by X-ray and NMR reveals the presence of naturally occurring stable intermediates whose PDB codes are 1DVR and 2BBW.[59] This gives strong support to the existence of I_N. In addition, intermediate I_L approximates the conformation of 1ZIN.[60] Very recently, the Bagchi group reported a stable intermediate called the "HOHC" (half-open

dx.doi.org/10.1021/ct300720s | J. Chem. Theory Comput. 2013, 9, 84−95

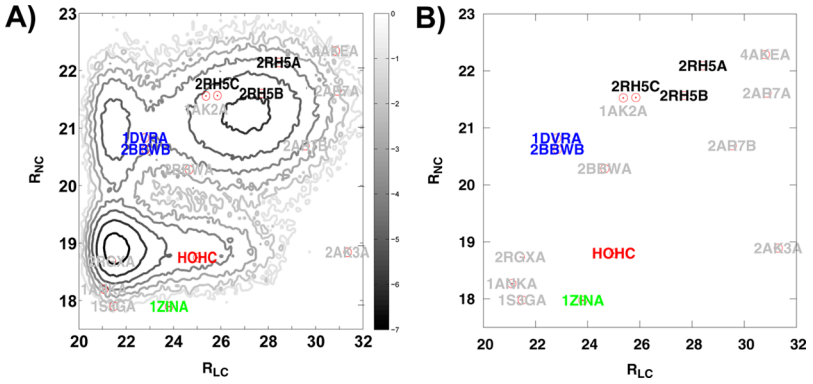

Figure 7. Comparison between predicted intermediates in our models with available experimental and theoretical structures. Relatively higher populated intermediate I_N seems to correspond to conformation B of 2BBW and conformation A of 1DVR. In addition, intermediate I_L approximates the conformational region of 1ZIN, especially for the conformation of "HOHC" (half-open half-closed) predicted by Bagchi group.

half-closed) state from the simulation of substrate-free ADK with explicit water solvents.[24] For the "HOHC" state, R_{LC} = 25 Å and R_{NC} = 18.8 Å. By comparison with the crystal structure (4AKE) in the open state in which R_{LC} = 30.8 Å and R_{NC} = 22.3 Å, and the crystal structure (1ANK) in the closed state in which R_{LC} = 21.0 Å and R_{NC} = 18.3 Å, it can be argued that the "HOHC" intermediate is indeed a state in which NMP is closed and LID is half-open or half-closed. From Figure 7, we can clearly see that the HOHC intermediate is perfectly consistent with I_L predicted by our model.[19] However, I_L in our model is not so stable, possibly because of the absence of protein−solvent interactions.[61,24] The possibility of intermediates existing is also evident by the fact that there are some additional non-noise signals from the single molecule FRET experiment.[10] Although the bimodal distribution with respect to a single RC in terms of the end to end distance previously extracted from the single molecule experimental data[13] did not seem to provide strong evidence of intermediates, it cannot rule out the existence of intermediates detected by our model. From our perspective, it is much easier to see the intermediate states with two RCs rather than one. Experimentally, this might be more challenging due to the multiple labeling of the additional fluorescence pair.

In 2007, Henzler-Wildman et al. reported an asymmetric crystal unit of apo ADK consisting of three different conformations whose PDB code is 2RH5.[10] By collating these structures and the fully closed conformation into a trajectory, they found that LID domains in these conformations lie between the fully open and fully closed conformation. By mapping the three crystal structures (2RH5A, 2RH5B, and 2RH5C) into the space of R_{LC} and R_{NC}, we can find that these conformations all belong to the conformational ensemble of the open state. The free energy profile reveals that the energy barriers for interconversion between these conformations are relatively low.

Which Pathway Is Dominant for Open↔Closed Transitions? Although there are abundant structures of ADK available, even making it possible to construct a movie of conformational change,[33,37,62] these structures cannot provide the order in which they are visited nor can they provide the pathway of conformational transitions. In ref 62, based on the movies constructed from available structures, the authors suggested two possible pathways for the conformation change. The two pathways were also observed in our simulation and previous works.[8,16,19,22,33,38,42] More importantly, the present model allows us to determine which pathway is predominant.

The prediction of intermediates by our model is highly consistent with the microscopic double-well model[19] in which the I_L pathway is dominating from both directions based on the rate analysis. In contrast, our model supports the conclusion that the I_N pathway is dominating for both directions based on the flux analysis.

By comparison with previous studies, for the closing direction, the dominant I_N pathway is supported by a number of studies.[16,20−22,32,33,37,38,42] However, for ADK opening, the I_N pathway is not well supported.[8,21] In addition, as an application of the implicit-ligand macroscopic double-well model, it was found that the conformation of ADK changed along the I_N pathway for the ligand-free model, however, along an alternate I_L pathway for the ligand-bound model.[21] In other words, such a model supports one single stepwise pathway in all cases and no intermediate. In contrast, our model reveals that the two pathways both play their roles in conformational change, and their weights can be modulated by external stimulations. In particular, we investigated the dependence of pathway weight and intermediate stability on temperature, ligand concentration, and binding affinity. It reveals that ligand binding increases the population of the closed state and a corresponding decrease in that of the open state. Additionally, AMP binding increases the weight of the I_L pathway and ATP binding favors I_N pathway. However, the mechanism of conformational change is relatively robust to the binding of ligands ATP and AMP. In contrast, the mechanism is highly sensitive to temperature. At the simulated temperature comparable with experimental room temperature, the I_N pathway is dominant. At the optimal temperature, the mechanism is reversed; that is, the I_L pathway is slightly dominant. At higher temperatures, the protein loses its activity dramatically because of the partial or full melting of two lids, making analysis of the pathway impossible.

Validation of Random Bi−Bi Model. About four decades ago, a random Bi−Bi mechanism was proposed to explain the order of binding and release of reactants for ADK via an isotope exchange experiment.[63] Such a mechanism is supported by a number of later experiments.[9,64] The introduction of explicit double natural substrates allows us to further observe the coupling of ligand dynamics with protein dynamics. From the results of model MT containing AMP and nonhydrolyzable ATP analog, we found that either substrate can bind first to the

dx.doi.org/10.1021/ct300720s | J. Chem. Theory Comput. 2013, 9, 84−95

enzyme and also can leave first. It corresponds to a classical random Bi−Bi mechanism. To the best of our knowledge, our work provides the first validation in the simulation.

Following the random Bi−Bi mechanistic framework, AMP binding and ATP binding should occur in a random order within the cell. Their binding and release are limited by the motion of the AMP lid and ATP lid. Opening of the lids is required for ligand binding. For the key catalytic step (not simulated in this work), it requires the closing of two lids for forming precise catalytic geometry. It is expected that, as AMP binds first, ADK closes its conformation along the NMP-closing-first pathway (I_L pathway). As ATP binds first, it will follow LID-closing-first pathway (I_N pathway). In principle, if the two natural substrates bind to ADK simultaneously, it will drive ADK to follow the direct pathway: LID and NMP close simultaneously (along the diagonal line in the two-dimensional free energy profile $F(Q_{LC},Q_{NC})$). Of course, we must acknowledge that the simultaneous closing of two lids is a rare event with very low possibility. The flux analysis has suggested that the direct fractional flux between O and C basins is below 0.1%. Overall, the random Bi−Bi model can provide a reasonable expection that the conformational change of the ADK enzyme very much follows two parallel stepwise pathways as a functional requirement for the double substrate catalysis. However, the classical random Bi−Bi model is not precise enough to describe the detailed mechanism. The cumulative data from computations and experiments can make the actual mechanism more clear.[9,16,19,64]

Which Lid's Movement Is the Rate-Limiting Step for the Conformational Cycle? There are abundant kinetic and thermodynamic experimental data available for ADK; however, the rate-limiting step still has yet to be determined. Even the kinetic experimental data are sometimes difficult to interpret in an unambiguous way. It was argued that from dynamic NMR dispersion experiments the large-scale conformational change associated with the LID opening motion is rate-limiting for the overall catalysis of the enzyme as noted in ref 17. However, we believe the data from dynamic NMR dispersion experiments[14] can only lead to the conclusion that the opening of the lids (AMP lid and ATP lid) is the rate-limiting step, but it is hard to pin down exactly which lid it is. Fortunately, the order or cooperativity of closure and opening for both the AMP and ATP lids can be investigated by single-molecule techniques, such as time-dependent FRET,[13] which has been applied in the study of ADK by Hanson et al. They monitored the conformational fluctuation by tracking the LID-CORE distance R_{LC}. Our simulation predicts that the opening of the AMP lid is the real rate-limiting step. This may be validated by experiments if more reaction coordinates such as the NMP-CORE distance can be introduced for monitoring the dynamics.

Population Shift or Induced Fit? Induced fit and population shift are two essential mechanisms for the description of the conformational change of the protein in the presence of ligands. However, the relative strengths of the two mechanisms for ADK as well as other proteins are still widely debated.[43,54] In the past, people believed that ADK changed its conformation in response to ligand binding, in line with the induced fit mechanism.[65,66] Recently, however, some people are inclined to the population shift mechanism[8,10,14−25,29,67] as a result of the discovery of the pre-existing closed conformation.[10,13,14,18,68] However, the pre-existence of the closed state does not necessarily indicate the working of the population shift mechanism. On the basis of the ligand-bound models, we found that there is no significant flux from the closed-unbound state to the closed-bound state. This finding rules out the population shift mechanism. Alternatively, this suggests an induced-fit type mechanism. In fact, the closed state cannot capture the ligands as the closure of lids which prevents ligands binding to their active sites.[69] We found that the population of the closed state shifted from 40% without ligands to 75% in the presence of AMP and ATP. This can be interpreted as the fact that ligand binding induces 35% of the open state to the closed state. From this standpoint, ADK should be put into the induced-fit category despite the fact that the closed conformation coexists with the open conformation in the free form of ADK.

Large-Scale Conformational Fluctuation Is an Intrinsic Property of ADK. On the one hand, free ADK enzymes demonstrate large-scale conformational fluctuations that encompass all of the conformations that are necessary for substrate binding and product release. On the other hand, the closed conformation sampled by free enzymes has no ability to capture ligands, which rules out the population shift mechanism. This could lead one to conclude that the highly populated closed state is "useless" and "superfluous". Why would ADK have to sample such a conformation even without ligands? Why would the energy landscape possess such a closed basin at the bottom beside the open basin, which is used for the only starting point of ligand binding?

We answer it by proposing that the large-scale conformational fluctuation is an intrinsic property of ADK. It is well established that free ADK has the ability to sample the closed state in previous works.[13] In fact, the FRET experiments also found that ADK had the ability to sample the open conformation with 6 times higher concentrations of ligands than that of the enzyme (3 mM AMP and ATP and 0.5 mM ADK enzyme). The present work further found that ADK has the ability to sample the open state in the presence of natural substrates, even with the highest concentrations, 14.7 mM. It has to be noted that we tuned the ligand concentrations by changing the effective volume of the simulated reaction container by a wall potential. The radius of the simulated container should not be less than the radius of gyration of the ADK enzyme. This leads to the highest concentration estimated to be 14.7 mM. This value should be higher if we consider the volume of the enzyme in the container. Therefore, our simulation results suggest that even under higher ligand concentrations than experimentally measured conditions close to saturated concentrations, both the open and closed conformational states still robustly coexist. The combination of these two findings strongly leads us to conclude that large-scale conformational fluctuation is an intrinsic property of ADK.

The intrinsic ability of ADK to sample large-scale conformational regions can facilitate catalytic cycles between the open conformation for capturing the reactants (AMP and ATP) and releasing the products (two ADPs) and the closed conformation for formation of the precise catalytic geometry. The existence of the on-pathway intermediates may further lower the barriers of conformational fluctuations and contribute to the enzyme catalytic cycle. In some cases, intermediates can work as traps to slow the dynamics. From the biological perspective, if ADK lacked such intrinsic conformational fluctuation under high substrate concentration (may be produced with a cell in a burst), it would run the risk of

becoming trapped in the closed state, leading the cell to lose its ability to catalyze AMP + ATP ↔ 2ADP and cellular homeostasis at large. Thus, the presence of large-scale conformational fluctuations are necessary for proper function. We also believe that the conformational intermediates, as well as the pathways between, are not random but rather a consequence of evolution.[30]

CONCLUSION

The relationship between structure, dynamics, and function is the key to understanding biomolecular interaction and recognition. The role of dynamics is challenging our understanding of enzyme catalysis, both experimentally and theoretically. There is also an important issue and debate on the interplay between functional dynamics and ligand binding. In this work, we developed a structure-based functional model with explicit ligands to explore the prototypical allosteric system, adenylate kinase. Our models predict two on-pathway intermediate states which link to stepwise parallel pathways on the functional landscape of ADK. Our double-ligand model MT further allows us to validate the random Bi−Bi reaction mechanism. Additionally, our present work strongly supports that the motion of the NMP domain is the rate-limiting step for enzyme turnover by flux description. It should be further investigated experimentally.

Furthermore, the present work demonstrates that ADK has the ability to sample the open state in the presence of natural substrates, even at peak concentration (several times the experimental saturated concentrations). Combined with previous works that have suggested that free ADK enzymes can sample the closed state, the two findings together strongly lead us to propose large-scale conformational fluctuations are an intrinsic property of ADK. Such intrinsic conformational fluctuation has the advantage of ADK avoiding being trapped in a deep basin in the energy landscape and causing a loss of function. We argue that the presence of intrinsic conformational fluctuations is a result of evolution, and is likely shared by other enzymes as well.

METHOD AND MATERIALS: COMPUTATIONAL DETAILS

Structure-based models have achieved widespread success in explaining the relationship between protein structure and folding behavior as a validation of energy landscape theory.[70] To extend the structure-based model to systems with multiple folding basins, we modified the traditional energy Hamiltonian by integrating information from the open and closed structures. In addition, for ligand-binding models, the ligand-related Hamiltonian is also included. The ligands introduced in our models contain both the AMP and ATP analogs (AMPPNP). Ligand−protein contacts for AMP- and ATP-bound models are extracted from PDB 1ANK. A wall potential was employed to switch models. On the basis of the fact that charged interactions have important roles in conformational dynamics[8] and ligand binding,[12] we introduced the electrostatic interactions using the Debye−Huckel model. Detailed descriptions of structure-based models can be found elsewhere.[70] Simulations were performed with Gromacs 4.0.5.[71] Reduced units were used for all calculations. A time step of 0.0005 time units (or ps) was used, and the simulation was coupled to a temperature bath via Langevin dynamics with a coupling time of 1.0. To ensure that the simulation is converged and the statistical errors are small enough, we simultaneously run several independent simulations using the same parameters set. See the SI for greater detail.

ASSOCIATED CONTENT

Supporting Information

Further details in the section Models and Methods and Figures S1−S12. This material is available free of charge via the Internet at http://pubs.acs.org.

AUTHOR INFORMATION

Corresponding Author

*E-mail: jin.wang.1@stonybrook.edu.

Notes

The authors declare no competing financial interest.

ACKNOWLEDGMENTS

We thank Haw Yang for critical reading of the manuscript. We thank Mr. Jeremy Adler for help in editing the manuscript. Y.W. is particularly grateful to Xiakun Chu and Feng Zhang for many helpful discussions. We thank the National Natural Science Foundation of China (Grant no. 21190040, 11174105) and National Science Foundation for their support. We acknowledge the High Performance Computing Center (HPCC) of Jilin University for supercomputer time.

REFERENCES

(1) Austin, R. H.; Beeson, K. W.; Eisenstein, L.; Frauenfelder, H.; Gunsalus, I. C. *Biochemistry* **1975**, *14*, 5355−73.
(2) Miyashita, O.; Onuchic, J. N.; Wolynes, P. G. *Proc. Natl. Acad. Sci. U.S.A.* **2003**, *100*, 12570−12575.
(3) Schug, A.; Onuchic, J. N. *Curr. Opin. Pharmacol.* **2010**, *10*, 709−714.
(4) Frauenfelder, H.; Sligar, S. G.; Wolynes, P. G. *Science* **1991**, *254*, 1598−603.
(5) Zhuravlev, P. I.; Papoian, G. A. *Q. Rev. Biophys.* **2010**, *43*, 295−332.
(6) Guo, W.; Shea, J. E.; Berry, R. S. *Ann. N.Y. Acad. Sci.* **2005**, *1066*, 34−53.
(7) Frauenfelder, H.; McMahon, B. H.; Austin, R. H.; Chu, K.; Groves, J. T. *Proc. Natl. Acad. Sci. U. S. A.* **2001**, *98*, 2370−4.
(8) Beckstein, O.; Denning, E. J.; Perilla, J. R.; Woolf, T. B. *J. Mol. Biol.* **2009**, *394*, 160−76.
(9) Tan, Y. W.; Hanson, J. A.; Yang, H. *J. Biol. Chem.* **2009**, *284*, 3306−13.
(10) Henzler-Wildman, K. A.; Thai, V.; Lei, M.; Ott, M.; Wolf-Watz, M.; Fenn, T.; Pozharski, E.; Wilson, M. A.; Petsko, G. A.; Karplus, M.; Hubner, C. G.; Kern, D. *Nature* **2007**, *450*, 838−44.
(11) Berry, M. B.; Meador, B.; Bilderback, T.; Liang, P.; Glaser, M.; Phillips, J. G. N. *Proteins* **1994**, *19*, 183−98.
(12) Berry, M. B.; Bae, E.; Bilderback, T. R.; Glaser, M.; Phillips, J. G. N. *Proteins* **2006**, *62*, 555−6.
(13) Hanson, J. A.; Duderstadt, K.; Watkins, L. P.; Bhattacharyya, S.; Brokaw, J.; Chu, J. W.; Yang, H. *Proc. Natl. Acad. Sci. U. S. A.* **2007**, *104*, 18055−60.
(14) Wolf-Watz, M.; Thai, V.; Henzler-Wildman, K.; Hadjipavlou, G.; Eisenmesser, E. Z.; Kern, D. *Nat. Struct. Mol. Biol.* **2004**, *11*, 945−9.
(15) Lou, H.; Cukier, R. I. *J. Phys. Chem. B* **2006**, *110*, 12796−808.
(16) Whitford, P. C.; Miyashita, O.; Levy, Y.; Onuchic, J. N. *J. Mol. Biol.* **2007**, *366*, 1661−71.
(17) Arora, K.; Brooks, r., C. L. *Proc. Natl. Acad. Sci. U. S. A.* **2007**, *104*, 18496−501.
(18) Aden, J.; Wolf-Watz, M. *J. Am. Chem. Soc.* **2007**, *129*, 14003−12.
(19) Lu, Q.; Wang, J. *J. Am. Chem. Soc.* **2008**, *130*, 4772−83.
(20) Liu, M. S.; Todd, B. D.; Sadus, R. J. *Aust. J. Chem.* **2010**, *63*, 405−412.

(21) Daily, M. D.; Phillips, J., G. N.; Cui, Q. *J. Mol. Biol.* **2010**, *400*, 618−31.
(22) Brokaw, J. B.; Chu, J. W. *Biophys. J.* **2010**, *99*, 3420−9.
(23) Bhatt, D.; Zuckerman, D. M. *J. Chem. Theory Comput.* **2010**, *6*, 3527−3539.
(24) Adkar, B. V.; Jana, B.; Bagchi, B. *J. Phys. Chem. A* **2011**, *115*, 3691−7.
(25) Nagarajan, S.; Amir, D.; Grupi, A.; Goldenberg, D.; Minton, A.; Haas, E. *Biophys. J.* **2011**, *100*, 2991−2999.
(26) Pirchi, M.; Ziv, G.; Riven, I.; Cohen, S. S.; Zohar, N.; Barak, Y.; Haran, G. *Nat. Commun.* **2011**, *2*, 493.
(27) Potoyan, D. A.; Zhuravlev, P. I.; Papoian, G. A. *J. Phys. Chem. B* **2012**, *116*, 1709−15.
(28) Matsunaga, Y.; Fujisaki, H.; Terada, T.; Furuta, T.; Moritsugu, K.; Kidera, A. *PLoS Comput. Biol.* **2012**, *8*, e1002555.
(29) Schrank, T. P.; Bolen, D. W.; Hilser, V. J. *Proc. Natl. Acad. Sci. U. S. A.* **2009**, *106*, 16984−9.
(30) Olsson, U.; Wolf-Watz, M. *Nat. Commun.* **2010**, *1*, 111.
(31) Jana, B.; Adkar, B. V.; Biswas, R.; Bagchi, B. *J. Chem. Phys.* **2011**, *134*, 035101.
(32) Franklin, J.; Koehl, P.; Doniach, S.; Delarue, M. *Nucleic Acids Res.* **2007**, *35*, W477−82.
(33) Maragakis, P.; Karplus, M. *J. Mol. Biol.* **2005**, *352*, 807−22.
(34) Pontiggia, F.; Zen, A.; Micheletti, C. *Biophys. J.* **2008**, *95*, 5901−12.
(35) Kubitzki, M. B.; de Groot, B. L. *Structure* **2008**, *16*, 1175−82.
(36) Snow, C.; Qi, G.; Hayward, S. *Proteins* **2007**, *67*, 325−37.
(37) Kantarci-Carsibasi, N.; Haliloglu, T.; Doruker, P. *Biophys. J.* **2008**, *95*, 5862−73.
(38) Li, W.; Wolynes, P. G.; Takada, S. *Proc. Natl. Acad. Sci. U.S.A.* **2011**, *108*, 3504−9.
(39) Daily, M. D.; Phillips, J., G. N.; Cui, Q. *PloS Comput. Biol.* **2011**, *7*, e1002103.
(40) Zuckerman, D. M. *J. Phys. Chem. B* **2004**, *108*, 5127−5137.
(41) Chu, J. W.; Voth, G. A. *Biophys. J.* **2007**, *93*, 3860−71.
(42) Whitford, P. C.; Gosavi, S.; Onuchic, J. N. *J. Biol. Chem.* **2008**, *283*, 2042−8.
(43) Wang, Y.; Tang, C.; Wang, E.; Wang, J. *Plos Comput. Biol.* **2012**, *8*, e1002471.
(44) Wang, J.; Wang, Y.; Chu, X.; Hagen, S. J.; Han, W.; Wang, E. *PLoS Comput. Biol.* **2011**, *7*, e1001118.
(45) Yao, X. Q.; Kenzaki, H.; Murakami, S.; Takada, S. *Nat. Commun.* **2010**, *1*, 117.
(46) Reinstein, J.; Vetter, I. R.; Schlichting, I.; Rosch, P.; Wittinghofer, A.; Goody, R. S. *Biochemistry* **1990**, *29*, 7440−50.
(47) Sinev, M. A.; Sineva, E. V.; Ittah, V.; Haas, E. *Biochemistry* **1996**, *35*, 6425−37.
(48) Bilderback, T.; Fulmer, T.; Mantulin, W. W.; Glaser, M. *Biochemistry* **1996**, *35*, 6100−6.
(49) Csermely, P.; Palotai, R.; Nussinov, R. *Trends Biochem. Sci.* **2010**, *35*, 539−546.
(50) Vertessy, B. G.; Orosz, F. *Bioessays* **2011**, *33*, 30−4.
(51) Boehr, D. D.; Nussinov, R.; Wright, P. E. *Nat. Chem. Biol.* **2009**, *5*, 789−96.
(52) Sinev, M. A.; Sineva, E. V.; Ittah, V.; Haas, E. *FEBS Lett.* **1996**, *397*, 273−6.
(53) Marinelli, F.; Pietrucci, F.; Laio, A.; Piana, S. *PLoS Comput. Biol.* **2009**, *5*, e1000452.
(54) Hammes, G. G.; Chang, Y. C.; Oas, T. G. *Proc. Natl. Acad. Sci. U. S. A.* **2009**, *106*, 13737−13741.
(55) Bhatt, D.; Zuckerman, D. M. *J. Chem. Theory Comput.* **2011**, *7*, 2520−2527.
(56) Li, W.; Terakawa, T.; Wang, W.; Takada, S. *Proc. Natl. Acad. Sci. U. S. A.* **2012**, *109*, 17770−1.
(57) Wang, Y.; Chu, X.; Suo, Z.; Wang, E.; Wang, J. *J. Am. Chem. Soc.* **2012**, *134*, 13755−13764.
(58) Best, R. B.; Chen, Y. G.; Hummer, G. *Structure* **2005**, *13*, 1755−1763.
(59) Schlauderer, G. J.; Proba, K.; Schulz, G. E. *J. Mol. Biol.* **1996**, *256*, 223−7.
(60) Berry, M. B.; Phillips, J., G. N. *Proteins* **1998**, *32*, 276−88.
(61) Fenimore, P. W.; Frauenfelder, H.; McMahon, B. H.; Parak, F. G. *Proc. Natl. Acad. Sci. U. S. A.* **2002**, *99*, 16047−16051.
(62) Vonrhein, C.; Schlauderer, G. J.; Schulz, G. E. *Structure* **1995**, *3*, 483−90.
(63) Rhoads, D. G.; Lowenstein, J. M. *J. Biol. Chem.* **1968**, *243*, 3963−72.
(64) Sheng, X. R.; Li, X.; Pan, X. M. *J. Biol. Chem.* **1999**, *274*, 22238−42.
(65) Pai, E. F.; Sachsenheimer, W.; Schirmer, R. H.; Schulz, G. E. *J. Mol. Biol.* **1977**, *114*, 37−45.
(66) Schulz, G. E. *Faraday Discuss.* **1992**, *93*, 85−93.
(67) Daily, M. D.; Makowski, L.; Phillips, G. N., Jr.; Cui, Q. *Chem. Phys.* **2012**, *396*, 84−91.
(68) Aden, J.; Verma, A.; Schug, A.; Wolf-Watz, M. *J. Am. Chem. Soc.* **2012**, *134*, 16562−16570.
(69) Sullivan, S. M.; Holyoak, T. *Proc. Natl. Acad. Sci. U. S. A.* **2008**, *105*, 13829−34.
(70) Clementi, C.; Nymeyer, H.; Onuchic, J. N. *J. Mol. Biol.* **2000**, *298*, 937−953.
(71) Hess, B.; Kutzner, C.; van der Spoel, D.; Lindahl, E. *J. Chem. Theory Comput.* **2008**, *4*, 435−447.